Journal of Orthopaedic Surgery and Research

RESEARCH ARTICLE Open Access

The one-in-all diagnostic value of ^{99m}Tc-MDP bone scan combining with single-photon emission tomography (SPECT)/CT imaging in spinal osteoblastoma

Wenhui Ma[1†], Zhiyong Quan[1†], Jing Wang[1], Xiangdong Li[2*] and Guoquan Li[1*]

Abstract

Background: Osteoblastoma (OB) is an intermediate lesion, which makes the accurate preoperative diagnosis very important. ^{99m}Tc-methylene diphosphonate (^{99m}Tc-MDP) bone scan and SPECT/CT imaging were evaluated for their diagnostic value in spinal OB.

Methods: This study was a retrospective analysis of patients with spinal OB lesions confirmed by pathology and diagnosed with bone scan and SPECT/CT for preoperative diagnosis from January 2008 to December 2018. The uptake levels of OB on planar bone scan were divided into low, medium, and high groups by visual assessment referring to the uptake of the normal rib, spine, and bladder. X-ray, CT, MRI, bone scan, and SPECT/CT imaging of the patients were analyzed for characteristics summary.

Results: Twenty-five patients were diagnosed for spinal OB (17 males and 8 females with a proportion of 2.1:1), and the average age was 26.8 ± 10.8 years (range 5~59). There were 8 lesions located in the cervical, 6 in the thoracic, and 11 in the lumbar vertebrae. Twenty-four lesions involved posterior elements, especially the pedicles (14/25). Symptoms were predominantly painful with a duration of 18.3 ± 13.9 months (range 0.5~60 months). The lesion size ranged from 9 to 35 mm. All the lesions were low to high uptake in the planar bone scan, and the percentages of low to high levels were 1 (4%), 8 (32%), and 16 (64%) cases.

Conclusions: Spinal OB mainly involved the posterior area, and elderly patients should be considered as well. SPECT/CT combined the characteristics of bone uptake and anatomical features of bone tumors, proving its one-in-all diagnostic value for spinal OB and other osteogenic tumors.

Keywords: Osteoblastoma, Bone scan, SPECT/CT

* Correspondence: xdlimail@yahoo.com; lgqby@sina.com
†Wenhui Ma and Zhiyong Quan contributed equally to this work.
[2]Department of Orthopedic Oncology, Xijing Hospital, Fourth Military Medical University, 127# West Changle Road, Xi'an 710032, Shaanxi Province, China
[1]Department of Nuclear Medicine, Xijing Hospital, Fourth Military Medical University, 127# West Changle Road, Xi'an 710032, Shaanxi Province, China

Introduction

Osteoblastoma (OB) is a rare and primary bone neoplasm which was first described by Jaffe and Lichtenstein in the 1950s, accounting for 1% of all primary bone tumors and around 3% of benign bone tumors [1–3]. OB is commonly located in the spine (35–50%) and usually in the posterior elements. Other frequently involved sites are the femur (16.4%), humerus (7%), and tibia (6%) [2]. OB is histological similar to osteoid osteoma (OO) but differs in size and more aggressive than OO biologically and can infiltrate extraskeletal tissues. When the diameter of lesions exceeds 1.5 cm, the diagnosis is highly suggestive of OB [4–6]. Malignant transformation in 12–25% of lesions has been described in the literature [7, 8]. Spinal OB most commonly affects the posterior aspects of the spine (laminae, pedicles, or spinous processes). The main clinical manifestations are of neurological nature and include progressive focal or radicular pain exacerbated by movement [6, 9]. Surgical resection is the main treatment method with high recurrence rates debated by the subtotal resection [10–12]. The effective treatment of spinal OB relies on precise diagnosis based on a crucial image. However, the radiographic features of OB can differ according to its location and type.

The diagnostic methods for spinal OB mainly include plain X-ray, computed tomography (CT), magnetic resonance imaging (MRI), and bone scan (BS). Plain radiography is usually the first diagnostic approach but has low sensitivity [13]. It often fails to reveal the tumor because of their relatively small size and complex anatomy around the vertebral column. The average delay in diagnosis is approximately 18–24 months in reports [7]. CT can present OB as a sclerotic or osteolytic expansive lesion with a central nidus and surrounding reactive soft tissue change. Sometimes, the presence of bone marrow and soft tissue changes of OB is characterized by a hypointense signal on T1-weighted sequence and high signal on T2-weighted in MRI, whereas ^{99m}Tc-methylene diphosphonate (^{99m}Tc-MDP) bone scan is commonly used in OB diagnosis because of its osteogenic feature, especially for those with ambiguous or negative radiographic results. It is especially helpful in children since the exact site of pain is difficult to elicit. However, the limitation of the planar bone scan results from false negative. It is hard to differentiate with another osteogenic disease especially in the diagnostic specificity and reduced sensitivity for bone marrow disease. Thus, the specificity of bone scan remains a concern.

By combining functional and anatomical information in a single imaging method, SPECT/CT gained widespread popularity in the last few years and has become a one-stop cancer imaging modality [14]. A few case reports have also demonstrated the usefulness of ^{99m}Tc-MDP SPECT/CT for the diagnosis of osteoid osteoma but not OB [15–17]. However, to date, there is no systematic study evaluating the utility of ^{99m}Tc-MDP SPECT/CT in spinal osteoblastoma. Therefore, we evaluated the role of SPECT/CT as a one-in-all imaging modality for the diagnosis of spinal OB in this study.

Materials and methods

Twenty-five patients were confirmed as spinal OB in histopathology and treated from January 2008 to December 2018. All procedures were in accordance with the ethics committee of Xijing Hospital and with the Helsinki Declaration of 1975 (revised in 2008). All patients were investigated by the following imaging resources performed in our hospital: plain X-rays, CT scan, MRI, bone scan, and SPECT/CT. Two experienced radiologists and nuclear medicine physicians reviewed the imaging results.

Radiotracer injection, planar bone scanning, and SPECT/CT acquisition

The patients were intravenously injected with ~ 10 MBq/kg (260–300 μCi/kg) of ^{99m}Tc-MDP for planar BS and SPECT/CT imaging. Images were acquired on SPECT/CT dual-head gamma camera (Symbia T2 or GE670, USA). Parallel-hole and low-energy high-resolution collimators were used with a 140-keV photopeak and a 20% symmetrical window. Delayed planar BS was performed 3~4 h after radiotracer injection. Anterior and posterior whole-body planar images were acquired in a continuous mode with the patient in the supine position (matrix 256 × 1024). The acquisition orbits of SPECT/CT were body contour orbits over 360° arcs, each of 6° for 60 stops. Emission data were acquired for 15 s per stop. The image acquisition matrix was 128 × 128.

Processing and analysis of images

All studies were uniformly processed with commercially available E.soft software (Siemens, USA) on a Syngo nuclear medicine workstation (Siemens, USA). SPECT images were reconstructed with the Flash-3D software (Siemens Medical Solutions, USA) with 8 subsets and 4 iterations. Subsequently, tomographic slices were generated and displayed as transaxial, coronal, and sagittal slices. SPECT emission images were co-registered and fused with CT images using the object versus the target matrix method.

Image interpretation

X-ray, CT, and MR images were evaluated by two experienced radiologists. The imaging features of the lesions were recorded such as tumor nidus, surrounding sclerosis, signal changes of the lesion, and surrounding tissues. Planar bone scan and SPECT/CT images were analyzed by two experienced nuclear medicine physicians. The readers were aware of the patients' clinical information but were blind to other imaging findings. The interpreters visually divided the relative uptake of lesions into four levels, negative uptake as the background, low

uptake as the ribs, medium uptake as the spine, and high uptake as the bladder (Fig. 1) [18]. For SPECT/ CT, OB was diagnosed based on abnormal focal uptake and SPECT along with specific features on CT.

Surgical treatment

The procedure was performed under general anesthesia. The surgical method (posterior approach, anterior approach, or combined approach) was selected based on the location and range of the lesion. The posterior approach (PA) was chosen if the lesion involved posterior elements of the spine, such as laminae, pedicles, or the transverse and spinous processes. Anterior approach (AA) and combined approach (AA+PA) should be taken into consideration if the lesion involved vertebral body. The treatment approach, length of stay, duration of the surgery, and blood loss were recorded.

Results

Patient characteristics

Twenty-five patients (17 males and 8 females) with a mean age of 26.8 ± 10.8 years (range, 5–59 years) were scanned with the ^{99m}Tc-MDP planar bone scan and SPECT/CT to detect spinal OB. Although 80~90% of cases are diagnosed before 30 years of age reported in the literature, 36% of patients (9/25) in our study were diagnosed after 30 years old. There were 8 lesions located in the cervical vertebra, 6 lesions in the thoracic vertebra, and 11 lesions in the lumbar vertebra. According to the location, OB usually involved the posterior area of the spine (24/25), especially in the pedicle of the vertebral arch (14/25). The symptom caused by OB was usually pain with or without numbness or weakness. The duration of the symptom was 18.3 ± 13.9 months (range, 0.5~60 months) depending on the lesion's location, treatment methods, and individual tolerance level. The characteristics of the patients were demonstrated in Table 1.

Imaging results

The imaging appearance of OB commonly mimics that of osteoid osteoma. However, it is usually larger in size (> 2 cm) and may have aggressive features according to the World Health Organization definitions published in 2013. The diameter of lesions in this study was from 9 to 35 mm. The imaging features with a detailed description of X-ray, CT, MRI, planar bone scan, and SPECT/CT were shown in Table 2.

The radiographic features in classic OB include a well-circumscribed, osteolytic-osteosclerotic lesion with an expansive, scalloped, or lobulated appearance. The detection of OB in the axial skeleton, complex anatomy, and adjacent articular region was limited on account of the superposition of other structures. Therefore, the imaging findings on X-ray usually included uneven density and expansive changes, making it difficult to distinguish from other lesions. CT is considered as the diagnostic modality of choice for tumor detection, which is based on the demonstration imaging features such as central nidus with surrounding sclerosis (Fig. 2). It could accurately show the extent of the lesion, presence or absence of matrix mineralization, location of the lesion (i.e., cortical or medullary) and surrounding bone changes. Sometimes there

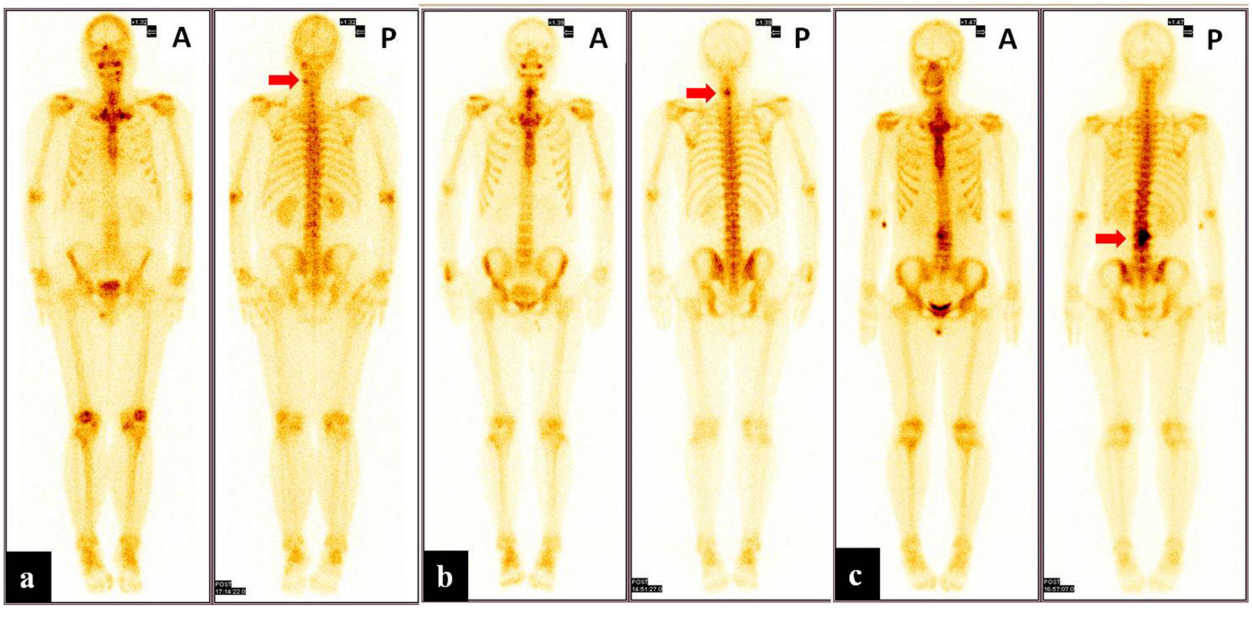

Fig. 1 Examples of spinal OB lesion (red arrow) uptake level on a planar bone scan. Low (**a**). Medium (**b**). High (**c**). A and P indicate the anterior and posterior imaging, respectively

Table 1 Patient demographics, location of spinal OB, symptoms, and duration of symptoms

No.	Sex	Age（ys）	Location		Symtoms	Duration of Symptoms(mo)
1	F	10	L4	RPV	night pain	6
2	M	31	T6	LPV+LTP+Rib	pain	36
3	M	23	L3	RPV	pain,numbness,weakness	24
4	M	30	C5	LLM	pain	24
5	M	27	T1	RPV	pain	36
6	M	40	C3	RPV	pain, numbness	0.5
7	M	9	C6	LPV	pain+paralysis	5
8	M	15	L3	RPV	pain	12
9	M	21	L2	LL	pain	24
10	M	16	L4	RPV	night pain	6
11	M	32	T7	LPV	pain increased after activity	36
12	F	20	L3	LPV	night pain	12
13	M	44	C5	LVB+LL+LPV+LTP+SP	No	0.5
14	F	54	C5	RVB	night pain	2
15	M	13	T6	RTP+RL+RPV+SP	pain	30
16	F	26	C3	LTP	weekness	60
17	M	28	C3-4	RTP+RL	night pain	27
18	M	19	L5	RIAP	pain	4
19	M	59	C1	LTP	pain	3
20	M	42	T10	LTP	pain	10
21	F	33	L2-3	RPV+RTP	pain	60
22	F	10	L5	RL	pain	20
23	F	26	L2	RVB+RPV	night pain	3
24	F	5	L4	RIAP	pain	24
25	M	37	L5	RPV	pain	1

LL/RL, left/right lamina; LLM, left lateral mass; LPV/RPV, left/right pedicle of the vertebral arch; LVB/RVB, left/right vertebral body; LTP/RTP, left/right transverse process; RIAP, right inferior articular process; SP, spinous processes.

is erosion of the cortex, and a common finding is the presence of a sclerotic rim representing a reaction from the bone and periosteum. MR may overestimate the aggressiveness of OB, due to the associated marked inflammation or edema illustrated as “flare response” (Fig. 2). MRI features were non-specific with typically low to isointense T1- and T2-weighted signal, decreased signal due to matrix calcification (if present), and intense enhancement representing the highly vascular nature of the lesion.

OB belongs to osteogenic lesions, and all 25 patients were found to have spinal lesions with positive ^{99m}Tc-MDP uptake (low~high level) result in BS (Table 2). The number of patients with low-, medium-, and high-level uptake in planar BS was 1 (4%), 8 (32%), and 16 (64%), respectively. SPECT/CT was a much more specific and valuable modality in the differential diagnosis of pathologic osseous conditions. The morphologic CT appearance of the scintigraphic positive lesion could achieve accurate differentiation between benign lesions and metastases based on the whole-body bone scan.

Malignant characteristics may occur in OB lesions sometimes, such as thinning, erosion of the cortex, and associated soft tissue mass. For example, patient no. 24 was diagnosed with tuberculosis based on CT with atypical

Table 2 Imaging findings with more specific descriptions of the abnormalities

No.	X-Ray	CT			MR	Bone scintigraphy	
		Nidus	Reactive Sclerosis	Diameter (cm)	Imaging discription	Planar image (Uptake Level)	SPECT/CT
1	Density reduction	Yes	Yes	1.2	/	Medium	Osteoblastoma
2	Expansive, uneven density	No	Yes	2.49	/	High	Osteoblastoma
3	/	No	Yes	2.2	/	High	Osteoblastoma
4	Increased density, narrowing of intervertebral space	Yes	Yes	2.2	/	Medium	Osteoblastoma
5	Uneven density	No	Yes	1.9	/	High	Osteoblastoma
6	/	No	No	2.4	/	Medium	Malignant lesions
7	/	No	Yes	1.3	/	High	Osteochondroma
8	/	No	No	1.9	/	High	Osteoblastoma
9	Uneven density	Yes	Yes	2.1	Expansive,hypointensive on T1	High	Osteoblastoma
10	Increased density	Yes	Yes	1.5	Hypointensive on T1, hyperintense on T2	Medium	Osteoblastoma
11	Uneven density, narrowing of intervertebral space,scoliosis	Yes	Yes	0.9	/	High	Osteiod Osteoma
12	/	No	Yes	2.2	/	High	Osteoblastoma
13	Uneven density, Spotted ossification	No	Yes	3.4	Expansive,Vertebral flattening,hyperintense on T2	Medium	Osteoblastoma
14	/	No	No	1.8	/	High	Metastatic lesion/Osteoblastoma
15	Normal	No	No	2.6	/	High	Aneurysmal bone cyst
16	Uneven density	No	Yes	1.9	Hyperintense on T2 in spinal marrow	High	Osteoblastoma/ osteofibrous dysplasia
17	Bone destruction and hyperplasia	Yes	Yes	2	Hypointensive on T1, inhomogeneous signal on T2, hyperintense on T2 in surrounding muscle	High	Osteoblastoma
18	/	No	Yes	2.5	/	Low	Osteoblastoma
19	/	No	Yes	1.9	/	High	Osteoblastoma
20	Expansive, density reduction	No	Yes	2.7	/	Medium	Osteoblastoma
21	Increased density	No	Yes	3.5	Hyperintensive on T1 and T2 in pedicle and spinous process of L2-3, Hyperintensive on T2 in transverse process	High	Osteoblastoma/ osteofibrous dysplasia
22	/	Yes	Yes	2	Hyperintensive on T1 and T2	High	Osteoblastoma
23	Increased density,osteosclerosis	No	No	2.4	Hypointensive on T1 and hyperintense on T2 in lesion and surrounding psoas muscle,obvious enhancement	High	Osteoblastoma
24	/	Yes	No	1.1	Lumbar vertebrae bent to the left	Medium	Osteiod Osteoma
25	Increased density, blur boundary	No	No	3.2	Hypointensive on T1 and hyperintense on T2 with obvious enhancement	Medium	Osteiod Osteoma

imaging features and unclear boundary with surrounding tissue. Meantime, MRI showed defects in the bone lesion and exaggerated peripheral response especially when the bone lesion was small, so the initial diagnosis was left lumbar curvature. Patient no. 17 (Fig. 3) and 21 displayed transverbrate lesions, indicating malignancy, which may also lead to a misdiagnosis as a metastatic lesion.

Surgical results

The symptoms, operative time, blood loss, and treatment approach of the patients were summarized in Table 3. The mean operative time was 202.0 ± 22.4 min (range, 120~360 min), and the average blood loss was 656.0 ± 428.2 mL (range, 100~4000 mL). The range of blood transfusion was 370~1420 mL. The mean length of hospital stay was 15.9 ± 5.8 days (range, 8~24 days). The symptoms of the pain were obviously relieved in the majority of the patients immediately after surgery. There were no leakage of cerebrospinal fluid, infectious complications, and neurological injury during the procedure. Histology confirmed OB in all patients after the surgery.

Discussion

Osteoblastoma occurs rarely in people older than 50 years of age, but sporadic cases of adulthood were described in the literature [2, 7, 19, 20]. In our study, four patients' age was older than 40 years old, and the oldest age was up to 59 years old. Therefore, OB is not a young person's exclusive illness. OB should be considered in the differential diagnosis of bone lesions of the spine in adulthood and in the elderly (which includes osteoblastic metastases like prostate and breast, vertebral hemangioma, osteochondroma, giant cell

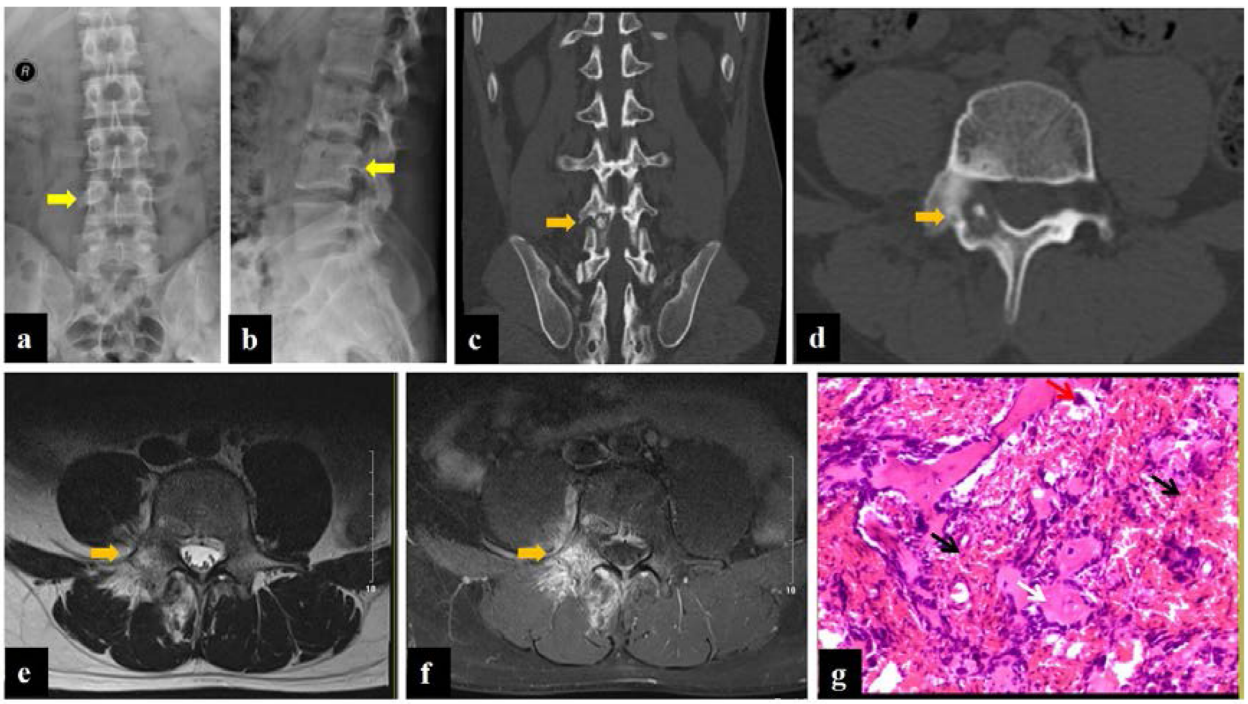

Fig. 2 Patient no. 10, male, 16 years old. Anteroposterior (**a**) and lateral (**b**) radiograph demonstrated the increased density in the right attachment of L4 (yellow arrow). CT (**c**, **d**) and MRI (**e**, **f**) of the lumbar spine represented a 15.4-mm lesion on the right vertebral arch of L4 with typical features of OB (orange arrow). Note the surrounding bone marrow and paraspinal soft tissue edema on T2W (**e**) and enhanced T1W/FS sequence (**f**), a typical finding of OB. The histopathology (**g**) displayed osteoblast (red arrow), bone-like tissue and woven bone (white arrow), and loose connective tissue rich in dilated small blood vessels (black arrow), indicating a diagnosis of OB

tumor, chondrosarcoma, chordoma, osteogenic sarcoma, or Paget disease) to reach a diagnosis rapidly and to avoid a delay in the definitive treatment.

CT is best for the observation of the fine structure, the intensity of cortical destruction, and the formation of a bone shell and soft tissue masses. A round or oval lytic lesion with soft tissue or hyperdense nidus surrounded by variable amounts of osteosclerosis was taken as positive imaging features for OB on CT [21]. According to our study, the spinal lesions usually involve the

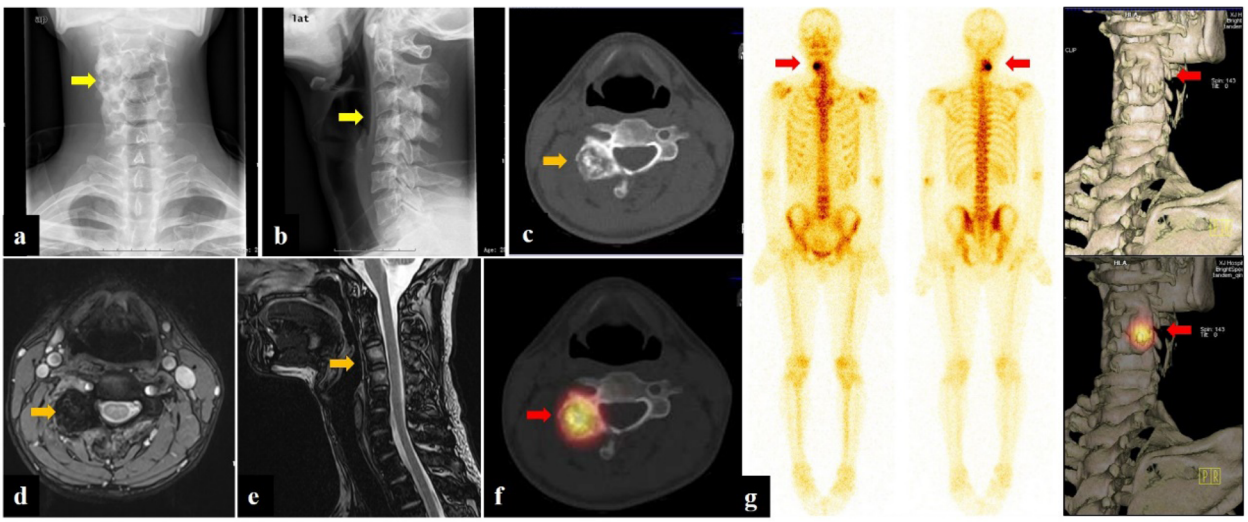

Fig. 3 Patient no. 10, male, 16 years old. Planar bone scan (**a**) demonstrated high uptake in the right attachment of the L4 level, indicating strong osteogenesis. SPECT/CT imaging (**b**) and 3D reconstruction images (**c**, **d**) clearly showed the center solid nidus with peripheral osteosclerosis

Table 3 Brief summary of spinal OB's surgical treatment

	Value
Length of stay (days)	15.9 ± 5.8
Duration of the procedure	202.0 ± 22.4
Blood loss	656.0 ± 428.6
Treatment approach	PA (23), PA + AA (2)
Red blood cell transfusion (IU)	4 ~ 10
Serum transfusion (mL)	370 ~ 1420

transverse process and the spinous process. OB cases (Fig. 4) may mimic malignancy, particularly when there was expansion, destruction of the bone cortex, new periosteal bone formation, or involving more than one vertebra. The aggressive nature of OB was also well illustrated in a study by Raskas et al., in which 56.6% of OB invaded the epidural space. However, the features occurred in none of 159 OO [22, 23]. If the radiologic findings suggest an aggressive lesion, biopsy should be done, including the periphery of the tumor or the cortical bone surrounding the tumor. MRI has a limited role in primary osseous tumors, because it poorly visualizes the bone marrow which can result in an inaccurate diagnosis of aggressive or malignant lesions [24]. Some patients were misdiagnosed with inflammatory diseases based on the less defined margin between osseous and soft tissues. Prevalent diffusion in young patients is probably due to the greater activity of osteoblasts, but the stromal component could explain the presentation.

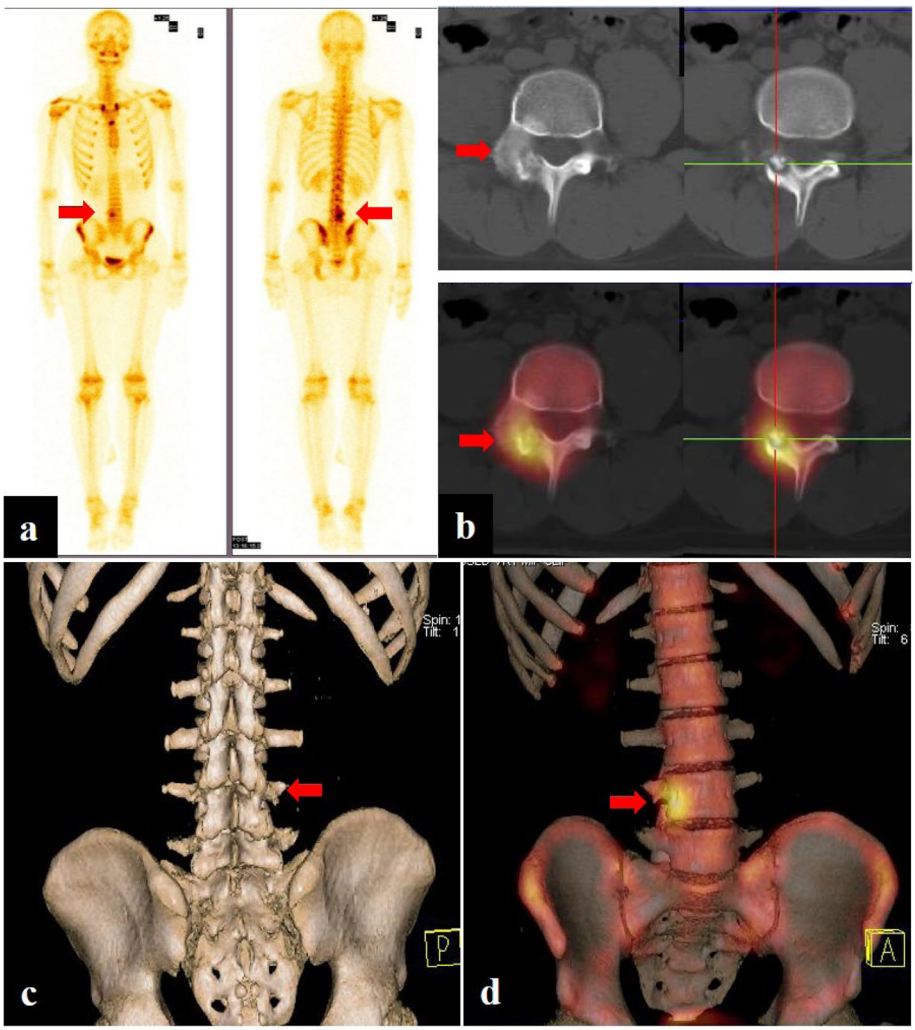

Fig. 4 Patient no. 17, male, 28 years old. Anteroposterior (**a**) and lateral (**b**) radiograph demonstrated bone destruction and hyperplasia in the C3–4 level (yellow arrow). CT (**c**) and MRI (enhanced T1W/FS and T2W sequence) (**d**, **e**) of the cervical spine showed a 20.0-mm lesion on the right transverse processes and laminae of C3–4, a typical osteogenic feature of OB (orange arrow). Planar bone scan displayed high uptake around C3–4 cervical vertebral body (**g**), whereas SPECT/CT (**f**) and 3D reconstruction images showed more details on the lesion and provided more information for orthopedist (red arrow)

Bone scintigraphy combined with CT or MRI becomes the most common method to diagnose and follow up skeletal metastases. However, using hybrid SPECT/CT can improve the specificity in cancer patients by accurately differentiating uptake between benign and malignant sites. Most patients with skeletal muscle metastases generally had markedly widespread involvement which led to an unusual appearance on SPECT/CT imaging. In spite of benign pathologic characteristics of OB, intense glucose metabolism of the tumor on FDG PET/CT suggested a malignancy [25]. Moreover, SPECT/CT provided an accurate identification of tumor viability that was useful for differential diagnosis, treatment planning, and follow-up. Osteoproliferative sclerosis needs to be differentiated from bone infection or osteosarcoma [26]. Both of them can be characterized by extensive bone sclerosis and involving soft tissue change. It was unique to find out whether there is a classical tumor nest. MRI showed a low or mixed signal and needs to be differentiated from chondroblastoma. When OB was associated with an aneurysmal bone cyst, it indicated a hybrid signal in MRI or mixed density on CT. Because of overlapping clinical and pathologic features between OB and OO, differential diagnosis is often unclear and difficult [27]. OB exacerbates pain that is non-responsive to non-steroidal anti-inflammatory drugs, and it usually—but not always—involves axial skeleton. There were certain defects in the lesions according to their diameter or size, such as unclear tumor boundaries, incomplete cortical bones or tumor infiltration through the intervertebral space into the spinal canal, fluid-level or secondary aneurysmal bone cysts, or lesions growing. Whether or not the diameter is bigger than 2 cm, OB should be considered. Aggressive behavior is within the biologic spectrum of OB, and histopathology alone does not appear to be a reliable predictor. Some patients may benefit from SPECT/CT in the following therapy.

The treatment option for OB mainly depends on its size and location. RFA is still a debatable procedure for the management of OB [28]. Surgery represents the first-line treatment in OB because it is the only strategy that ensures complete disease healing. Surgery decreases the risk of local recurrence and enables us to offer the best quality of life in correlation with life expectancy considering the fact that it mainly afflicts young people [29]. Since this study was a retrospective analysis, the incomplete data and low incidence rate of OB made a large number of studies necessary in the future. However, orthopedic oncology surgeons become more and more dependent on the accurate diagnoses of bone tumors with planar scanning and SPECT/CT.

Conclusions

Spinal OB mainly involved the posterior area, and middle-aged or elderly patients should be considered as well. SPECT/CT combined the characteristics of bone uptake and anatomical features of bone tumors, indicating an excellent way for one-in-all diagnosis and differentiation of spinal OB and other osteogenic tumors. With the popularity of SPECT/CT, it will show great potential for diagnosing the ambiguous bone disease and be helpful for further treatment in the future.

Abbreviations

^{99m}Tc-MDP: ^{99m}Tc-methylene diphosphonate; AP: Anterior approach; BS: Bone scan; CT: Computed tomography; MRI: Magnetic resonance imaging; OB: Osteoblastoma; OO: Osteoid osteoma; PA: Posterior approach; RFA: Radiofrequency ablation; SPECT: Single-photon emission tomography

Acknowledgements

This work was supported by the National Natural Science Foundation of China (Grant No. 81601521). The authors wish to thank Guiyu Li, Keke Xin, and Zhiping Yang from the Fourth Military Medical University for the image work.

Authors' contributions

Wenhui Ma was mainly working on the imaging analysis and writing of the manuscript. Zhiyong Quan and Jing Wang took charge of the data collection. Xiangdong Li and Guoquan Li were responsible for designing and reviewing the manuscript. The author(s) read and approved the final manuscript.

Ethics approval and consent to participate

All procedures were in accordance with the ethics committee of Xijing Hospital and with the Helsinki Declaration of 1975 (revised in 2008).

Consent for publication

All authors have approved for the publication.

Competing interests

The authors declare no competing financial interest.

Received: 23 October 2019 Accepted: 27 March 2020
Published online: 24 May 2020

References

1. Lichtenstein L. Benign osteoblastoma; a category of osteoid-and bone-forming tumors other than classical osteoid osteoma, which may be mistaken for giant-cell tumor or osteogenic sarcoma. Cancer. 1956;9(5):1044–52.
2. Yalcinkaya U, Doganavsargil B, Sezak M, Kececi B, Argin M, Basdemir G, Oztop F. Clinical and morphological characteristics of osteoid osteoma and osteoblastoma: a retrospective single-center analysis of 204 patients. Ann Diagn Pathol. 2014;18(6):319–25.
3. Li Z, Zhao Y, Hou S, Mao N, Yu S, Hou T. Clinical features and surgical management of spinal osteoblastoma: a retrospective study in 18 cases. PLoS One. 2013;8(9):e74635.
4. Chotel F, Franck F, Solla F, Dijoud F, Kohler R, Berard J, Abelin Genevois K. Osteoid osteoma transformation into osteoblastoma: fact or fiction? Orthop Traumatol Surg Res. 2012;98(6 Suppl):S98–104.
5. Youssef BA, Haddad MC, Zahrani A, Sharif HS, Morgan JL, al-Shahed M, al-Sabty A, Choudary R. Osteoid osteoma and osteoblastoma: MRI appearances and the significance of ring enhancement. Eur Radiol. 1996;6(3):291–6.
6. Samdani A, Torre-Healy A, Chou D, Cahill AM, Storm PB. Treatment of osteoblastoma at C7: a multidisciplinary approach. A case report and review of the literature. Eur Spine J. 2009;18(Suppl 2):196–200.
7. Boriani S, Amendola L, Bandiera S, Simoes CE, Alberghini M, Di Fiore M, Gasbarrini A. Staging and treatment of osteoblastoma in the mobile spine: a review of 51 cases. Eur Spine J. 2012;21(10):2003–10.
8. Weber MA, Sprengel SD, Omlor GW, Lehner B, Wiedenhofer B, Kauczor HU, Rehnitz C. Clinical long-term outcome, technical success, and cost analysis of radiofrequency ablation for the treatment of osteoblastomas and spinal

osteoid osteomas in comparison to open surgical resection. Skeletal Radiol. 2015;44(7):981–93.
9. Lucas DR. Osteoblastoma. Arch Pathol Lab Med. 2010;134(10):1460–6.
10. Marsh BW, Bonfiglio M, Brady LP, Enneking WF. Benign osteoblastoma: range of manifestations. J Bone Joint Surg Am. 1975;57(1):1–9.
11. Harrop JS, Schmidt MH, Boriani S, Shaffrey CI. Aggressive "benign" primary spine neoplasms: osteoblastoma, aneurysmal bone cyst, and giant cell tumor. Spine (Phila Pa 1976). 2009;34(22 Suppl):S39–47.
12. Galgano MA, Goulart CR, Iwenofu H, Chin LS, Lavelle W, Mendel E. Osteoblastomas of the spine: a comprehensive review. Neurosurg Focus. 2016;41(2):E4.
13. Greenspan A. Benign bone-forming lesions: osteoma, osteoid osteoma, and osteoblastoma. Clinical, imaging, pathologic, and differential considerations. Skeletal Radiol. 1993;22(7):485–500.
14. Abikhzer G, Keidar Z. SPECT/CT and tumour imaging. Eur J Nucl Med Mol Imaging. 2014;41(Suppl 1):S67–80.
15. Hephzibah J, Theodore B, Oommen R, David K, Moses V, Shah S, Panicker J. Use of single-photon emission computed tomography/low-resolution computed tomography fusion imaging in detecting an unusually presenting osteoid osteoma of the lumbar vertebra. Am J Orthop (Belle Mead NJ). 2009;38(3):117–9.
16. Farid K, El-Deeb G, Caillat Vigneron N. SPECT-CT improves scintigraphic accuracy of osteoid osteoma diagnosis. Clin Nucl Med. 2010;35(3):170–1.
17. Xing Y, Zhao J, Wang T. A case of paranasal sinuses osteoma detected on bone SPECT/CT. Clin Nucl Med. 2011;36(3):224–6.
18. Helms CA. Osteoid osteoma. The double density sign. Clin Orthop Relat Res. 1987;222:167–73.
19. Jiang L, Liu XG, Wang C, Yang SM, Liu C, Wei F, Wu FL, Zhou H, Dang L, Liu ZJ. Surgical treatment options for aggressive osteoblastoma in the mobile spine. Eur Spine J. 2015;24(8):1778–85.
20. Lucas DR, Unni KK, McLeod RA, O'Connor MI, Sim FH. Osteoblastoma: clinicopathologic study of 306 cases. Hum Pathol. 1994;25(2):117–34.
21. Flemming DJ, Murphey MD, Carmichael BB, Bernard SA. Primary tumors of the spine. Semin Musculoskelet Radiol. 2000;4(3):299–320.
22. Hladky JP, Lejeune JP, Singer B, Lecomte-Houcke M, Herbaux B, Dhellemmes P. Osteoblastoma of the odontoid process. Pediatr Neurosurg. 1994;21(4):260–2.
23. Cheung FM, Wu WC, Lam CK, Fu YK. Diagnostic criteria for pseudomalignant osteoblastoma. Histopathology. 1997;31(2):196–200.
24. Davies M, Cassar-Pullicino VN, Davies AM, McCall IW, Tyrrell PN. The diagnostic accuracy of MR imaging in osteoid osteoma. Skeletal Radiol. 2002;31(10):559–69.
25. Jeong YJ, Sohn MH, Lim ST, Kim DW, Jeong HJ, Jang KY, Yim CY. Osteoblastoma in the nasal cavity: F-18 FDG PET/CT and Tc-99 m MDP 3-phase bone scan findings with pathologic correlation. Clin Nucl Med. 2011; 36(3):214–7.
26. Yin H, Zhou W, Yu H, Li B, Zhang D, Wu Z, Liu T, Xiao J. Clinical characteristics and treatment options for two types of osteoblastoma in the mobile spine: a retrospective study of 32 cases and outcomes. Eur Spine J. 2014;23(2):411–6.
27. Barlow E, Davies AM, Cool WP, Barlow D, Mangham DC. Osteoid osteoma and osteoblastoma: novel histological and immunohistochemical observations as evidence for a single entity. J Clin Pathol. 2013;66(9):768–74.
28. Stavridis SI, Pingel A, Schnake KJ, Kandziora F. Diagnosis and treatment of a C2-osteoblastoma encompassing the vertebral artery. Eur Spine J. 2013; 22(11):2504–12.
29. Charles YP, Schuller S, Sfeir G, Steib JP. Cervical osteoblastoma resection and posterior fusion. Eur Spine J. 2014;23(3):711–2.

Publisher's Note